Materials Letters 255 (2019) 126569

Contents lists available at ScienceDirect

Materials Letters

journal homepage: www.elsevier.com/locate/mlblue

Ion implantation inducing two-way shape memory effect in Cu-Al-Ni thin films

M. Morán [a,b,*], A.M. Condó [a,b], S. Suárez [a,b], F. Soldera [c], N. Haberkorn [a,b]

[a] Comisión Nacional de Energía Atómica and Consejo Nacional de Investigaciones Científicas y Técnicas, Centro Atómico Bariloche, Av. Bustillo 9500, 8400 San Carlos de Bariloche, Argentina
[b] Instituto Balseiro, U. Nacional de Cuyo, Bustillo 9500, S. C. de Bariloche, Argentina
[c] Department of Materials Science & Engineering, Saarland University, D-66123 Saarbrücken, Germany

ARTICLE INFO

Article history:
Received 5 August 2019
Received in revised form 20 August 2019
Accepted 21 August 2019
Available online 22 August 2019

Keywords:
Thin films
Irradiation
Shape memory alloys
Cu-Al-Ni

ABSTRACT

We report two-way shape memory effect (TWSME) induced by Al ion implantation in 6 μm thick Cu-Al-Ni thin films. The films display an average grain size of 3.7 μm and a martensitic transformation temperature (M_S) of ≈ 240 K. The film was irradiated with 2 MeV Al ions with a fluence of 6×10^{15} ion.cm^{-2} (penetration distance up to ≈ 1.1 μm). After irradiation, the film displays well defined TWSME with a radius of curvature of ≈ 1 mm. The results indicate that the irradiation produces mainly changes in the austenitic order.

1. Introduction

Shape memory alloys (SMA) display the capacity to restore their original dimensional integrity (pre-deformed shape and size) after undergoing substantial deformation when heated to a certain temperature. The effect is related to a structural phase transition (martensitic transformation, MT) from high-temperature austenite to low-temperature martensite [1]. SMA are attractive materials for applications in the micro-electro-mechanical system (MEMS) due to the so-called two-way shape memory effect (TWSME) [2,3]. The latter refers to a reproducible change into two defined shapes during thermal cycling. It is not intrinsic of SMA but may be induced by thermomechanical training (bulk) and surface treatments (thin films) [2–4].

Cu–Al–Ni is an SMA which have the capability to be used both as sensors and actuators at temperatures going from tens of Kelvins to 473 K [5]. The MT is affected by the chemical composition [5], the order degree [6] and the microstructure [7,8]. Cu-Al-Ni display two possible kinds of martensite structures: γ'_3 (orthorhombic, 2H) and β'_3 (monoclinic, 18R) [9]. During the quenching treatment usually employed to avoid precipitation of equilibrium phases, the metastable disordered phase (β) of Cu-Ni-Al undergoes two successive order–disorder transitions: B2 (*Pm3m*) and $L2_1$ (*Fm3m*) ordering, respectively. Moreover, the order degree depends on the cooling rate of the quenching treatment and evolves during thermal aging [10]. In addition, irradiation with high energy particles can alter the phase stability [4,11]. Regarding applications in MEMS, Cu-Al-Ni nanopillars display super-elasticity [12] and thin films exhibit MT [13–15]. As in bulk, the hysteresis in the MT of thin films is strongly affected by grain boundaries. Thin films with micrometric grain size display hysteresis $\Delta h \approx 30$ K. Moreover, the MT is not influenced by superficial passivation layers [13]. The latter implies that it is possible to add a biocompatible material at the surface. Unlike NiTi [2–4], the TWSME in Cu-Al-Ni thin films has not been reported.

This letter reports TWSME induced by Al ion implantation in 6 μm thick Cu-Al-Ni thin films with micrometric grain size [13]. The irradiation was performed with 2 MeV Al ions and fluence 6×10^{15} ion.cm^{-2}. The energy was selected to generate a gradient of defects and implantation of Al at a typical distance of ≈ 1.1 μm from the surface. We analyze the presence of TWSME and the influence of the irradiation on the microstructure.

2. Experimental methods

The films were grown by DC sputtering on Highly Ordered Pyrolytic Graphite HOPG (0001) at 870 K [13]. The deposition parameters were: an atmosphere of 10 mtorr of Ar, an applied power of 50 W and a distance target/substrate of 7 cm. The

* Corresponding author.
E-mail address: mjmoran@cab.cnea.gov.ar (M. Morán).

https://doi.org/10.1016/j.matlet.2019.126569
0167-577X/

chemical composition of the target was Cu–27.35 at.% Al–5.45 at.% Ni (M_S = 240 K and $\Delta h \approx 10$ K). After growth, the films were cooled down in vacuum by turning off the heater. Under this procedure, the microstructure displays coexistence of austenite $L2_1$, and α (Cu) and γ_2 (Cu_9Al_4) equilibrium phases. Next, the films, with a typical size of 1 cm^2, were peeled off from the substrate and encapsulated in quartz tubes under an atmosphere of argon (inside a tantalum envelope). Thermal annealing was performed at 1123 K for 30 min [16]. After the annealing process, the samples were fast quenched in an ice-water mixture.

The microstructure of the film was studied by transmission electron microscopy (TEM) using an FEI Tecnai F20 UT microscope. Selected area electron diffraction (SAED) patterns in the TEM were acquired with a Gatan GIF Quantum ER energy filter. Cross-section TEM samples were prepared by using a focused ion beam (FIB) SEM dual beam FEI Helios NanoLab 600 equipped with an Omniprobe 100 micromanipulator. The MT was characterized by electrical transport using a conventional four-probe geometry. Irradiation with 2 MeV Al ions was performed with a 1.7 MV TANDEM particle accelerator. The fluence was selected in 6×10^{15} ion.cm^{-2} (total time 9 min). The range of penetration was obtained from a SRIM-TRIM simulation [17]. The energy of the ions was selected to generate a profile of disorder and implantation of the Al ions close to one of the surfaces.

3. Results and discussion

The microstructure of the Cu-Al-Ni films has been reported in ref. [15]. The films display grain size average $D \approx 3.7$ μm with an MT to an 18R structure. The M_s depends on chemical composition and order degree. The hysteresis is ≈ 27–30 K. Fig. 1a shows the damage profile created in the film by 2 MeV Al ions. Most of the damage occurs ≈ 1.1 μm below the surface, in a limited range of depth at the end of the ion's flight path (Bragg peak). The reduction in M_s due to the change in the chemical composition produced by Al addition is smaller than 0.1 K [5]. Fig. 1b shows resistance versus temperature for a film before and after irradiation. The results indicate that M_s increases from ≈ 210 K to 240 K with irradiation. Moreover, there is an unexpected small reduction in Δh and a smaller change in the jump at the normalized resistivity. For the irradiated film, the austenite is fully recovered at $A_f \approx 270$ K. We attribute the changes in M_s to an increment in the $L2_1$ degree of order produced by heating on the overall sample inherent to the irradiation process [13]. The differences in resistivity may be related to reduction in the transformed fraction or to changes in the twin boundary structure.

Usually, unirradiated films display shape memory effect. When the film is deformed in martensite, flat shape is recovered in austenite [11]. Fig. 2 shows the sequence of images when the irradiated film is thermally cycled in a liquid nitrogen vapor source. The film displays TWSME without any mechanically induced deformation. The film curves on the irradiated surface (top surface). Starting from room temperature (Fig. 2a), the film deforms to buckle when is cooled down (Fig. 2b and c) and recover the original shape when it is warming up to room temperature (Fig. 2a and d). The process is completely reproducible (sequence of images in Supplementary material). The radius of curvature at the martensitic phase is ≈ 1 mm.

To understand the influence of the irradiation on the austenitic phase, we study the microstructure by TEM. Fig. 3a shows a TEM bright field cross-section image of an irradiated Cu-Al-Ni film. The dark grain corresponds to austenite oriented along the $[1\bar{1}0]$ zone axis. The arrow indicates the direction perpendicular to the irradiated surface. The circles correspond to regions in which we obtain SAED patterns at different surface distances. Typical SAED for the regions at distances of 0.4 μm and 1.9 μm, and a key diagram are shown in Fig. 3b–d, respectively. There are not crystalline defects that can be directly related to the influence of the ion implantation. To analyze the influence of the irradiation on the

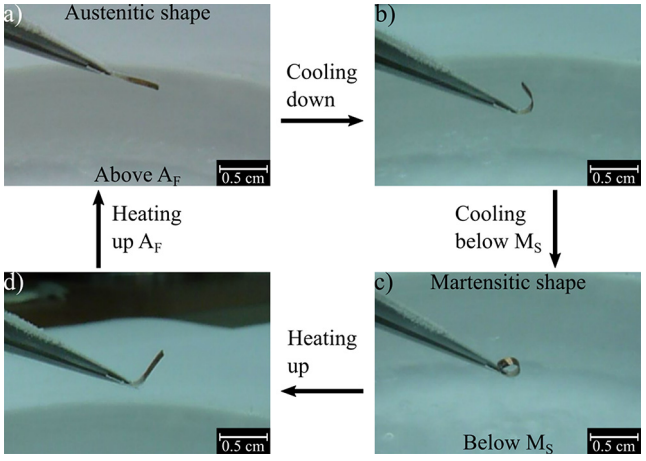

Fig. 2. TWSME in a Cu-Al-Ni film irradiated with Al ions and a fluence of 6×10^{15} ion.cm^{-2}. *a)* Room temperature austenite. *b)* Transforming from austenite to martensite during the cooling down in a gradient of temperature (vapor of N_2). *c)* Low temperature martensite. *d)* Transforming from martensite to austenite. The two-way shape memory is reproducible.

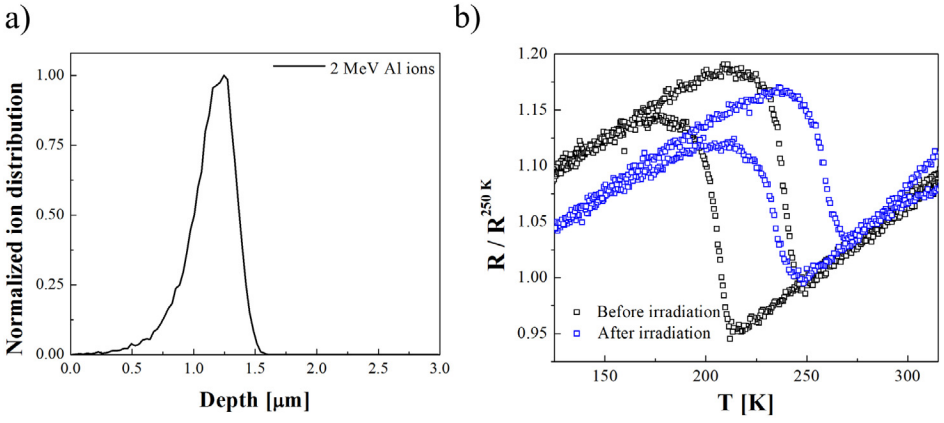

Fig. 1. *a)* SRIM-TRIM simulations showing the effective range (penetration) of 2 MeV Al ions in the Cu-Al-Ni alloy. *b)* Temperature dependence of the normalized resistance ($R/R^{250\ K}$) for 6 μm thick Cu-Al-Ni films before and after irradiation.

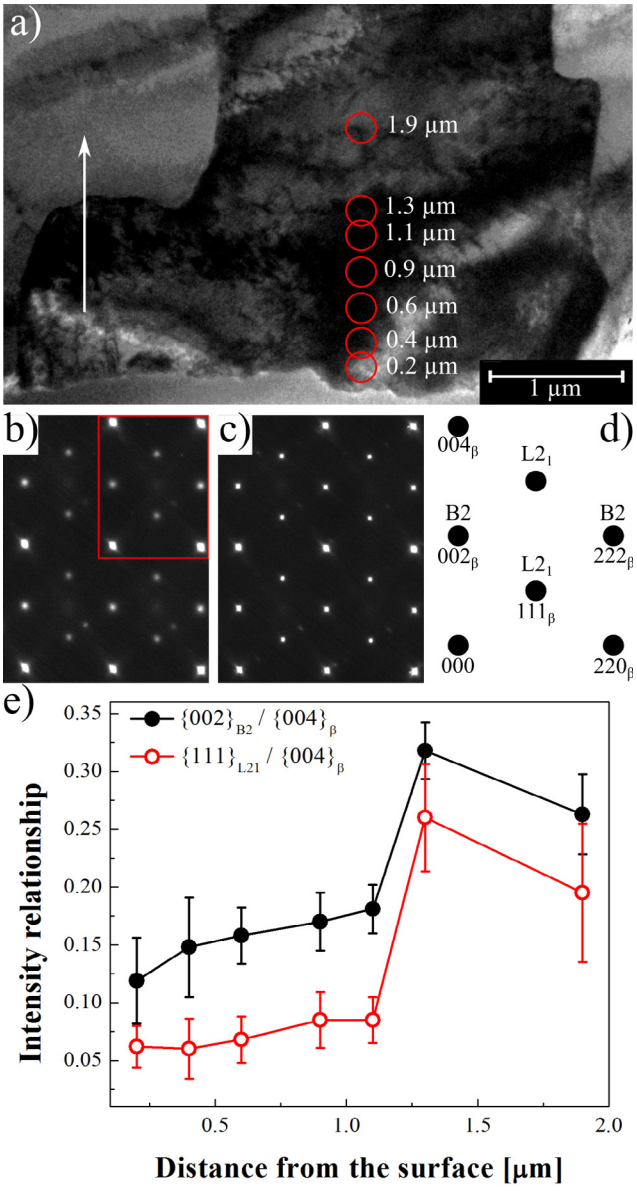

Fig. 3. *a)* TEM bright field cross section image of an irradiated Cu-Al-Ni film. Circles indicate region corresponding to SAED. *b-c)* Typical SAED for the regions at 0.4 y 1.9 μm. *d)* Key diagram of the top right hand part of patterns in (*b*) and (*c*); B2 and $L2_1$ superlattice spots are indicated. *e)* Profile in-depth of the intensity relationship of the superlattice spots $\{0\,0\,2\}_{B2}$ and $\{1\,1\,1\}_{L21}$ normalized by the intensity of the spot $\{0\,0\,4\}_{\beta}$.

order degree in the austenitic phase, we measure the intensity of the superlattice spots $\{1\,1\,1\}_{L21}$ and $\{0\,0\,2\}_{B2}$ normalized by that corresponding to the spots $\{0\,0\,4\}_{\beta}$ within the same pattern. The SAED patterns were obtained with the zero loss peak to avoid intensity from inelastic background. Fig. 3e shows a profile of their normalized intensity as a function of the distance to the irradiated surface. The results show that the irradiation strongly reduces the degree of order in the austenite. The influence of the disorder on the MT has been previously discussed in Refs. [18] and [19]. The changes in the degree of order in the nearest neighbor and next-nearest neighbor for Cu-Al-Ni have counter-effect. Increase the order from β to B2 decrease M_s. On the other hand, an increment in the $L2_1$ order increases M_s. A similar effect, but in the opposite direction, should takes place by irradiation. Comparing the MT before and after irradiation, it is clear that the $L2_1$ order increases in the non-irradiated regions (related to the heating produced by the irradiation). A probable explanation for the TWSME is that the profile of disorder produced by the irradiation modifies the twin boundary structure and the transformed volume. Although no changes in the type of martensite are expected due to the negligible addition of Al [5], the martensite structure may be affected by the disorder. For example, plastically deformed Cu-Al-Ni displays coexistence of β'_3 and γ'_3 structures [8]. The latter appears as a consequence of its preferential nucleation due to internal stresses [20].

4. Conclusions

In summary, we report Al ion irradiation/implantation inducing TWSME in Cu-Al-Ni thin films with micrometric grain size. The effect is reproducible in several thermal cycling. The radius of curvature in the buckle is ≈ 1 mm. The effect can be related with changes in the degree of order in the austenite modifying the twin structure. The possibility to tune M_s over a wide range of temperatures and TWSME makes Cu-Al-Ni thin films promising for application in microactuators such as microwrappers.

Declaration of Competing Interest

The authors declare that they have no known competing financial interests or personal relationships that could have appeared to influence the work reported in this paper.

Acknowledgment

We thank C. Olivares for technical assistance. M. M. and N. H. are members of the Instituto de Nanociencia y Nanotecnología, CNEA-CONICET (Argentina).

Appendix A. Supplementary data

Supplementary data to this article can be found online at https://doi.org/10.1016/j.matlet.2019.126569.

References

[1] K. Otsuka, X. Ren, Mater. Sci. Eng. A 273 (1999) 89–105, https://doi.org/10.1016/S0921-5093(99)00291-9.
[2] Fu. Yongqing et al., Sens. Actuat. A 112 (2004) 395–408, https://doi.org/10.1016/j.sna.2004.02.019.
[3] Nitin Choudhary, Davinder Kaur, Sens. Actuat. A Phys. 242 (2016) 162–181, https://doi.org/10.1016/j.sna.2016.02.026.
[4] David S. Grummon, Rolf Gotthardt, Acta Mater. 48 (2000) 635–646, https://doi.org/10.1016/S1359-6454(99)00401-2.
[5] V. Recarte et al., Mater. Sci. Eng. A 273–275 (1999) 380–384, https://doi.org/10.1016/S0921-5093(99)00302-0.
[6] V. Recarte, O.A. Lambri, R.B. Pérez-Sáez, Appl. Phys. Lett. 70 (1997) 3513–3515, https://doi.org/10.1063/1.119217.
[7] P. La Roca et al., Scr. Mater. 135 (2017) 5–9, https://doi.org/10.1016/j.scriptamat.2017.03.016.
[8] B.B. Straumal et al., Acta Mater. 125 (2017) 274–285, https://doi.org/10.1016/j.actamat.2016.12.003.
[9] V. Recarte et al., Metall. Mater. Trans. A 33 (2002) 2581–2591, https://doi.org/10.1007/s11661-002-0379-8.
[10] V. Recarte et al., J. Mater. Res. 14 (1999) 2806–2813, https://doi.org/10.1557/JMR.1999.0375.
[11] A. Tolley, C. Abromeit, Scr. Metall. Mater. 32 (1995) 925–930, https://doi.org/10.1016/0956-716X(95)93226-T.
[12] J. San Juan, M.L. Nó, C.A. Schuh, Acta Mater. 60 (2012) 4093–4106, https://doi.org/10.1016/j.actamat.2012.04.021.
[13] M.J. Moran et al., Mater. Lett. 184 (2016) 177–180, https://doi.org/10.1016/j.matlet.2016.08.027.
[14] M. Morán, A.M. Condo, N. Haberkorn, Mater. Charact. 139 (2018) 446–451, https://doi.org/10.1016/j.matchar.2018.03.025.
[15] M. Morán et al., Mater. Res. Exp. 6 (2019), https://doi.org/10.1088/2053-1591/ab2fbf 096556.

[16] S. Miyazaki, K. Otsuka, ISIJ Int. 29 (1989) 353–377, https://doi.org/10.2355/isijinternational.29.353.
[17] J.F. Ziegler, J.P. Biersack, U. Littmark, The Stopping and Range of Ions in Solids, Pergamon, New York, 1985.
[18] J. Van Humbeeck, L. Delaey, M. Chandrasekaran, ISIJ Int. 29 (1989) 388–394, https://doi.org/10.2355/isijinternational.29.388.
[19] V. Recarte et al., J. Appl. Phys. 86 (1999) 5467–5473, https://doi.org/10.1063/1.371547.
[20] M.L. Nó et al., Acta Mater. 52 (2010) 6181–6193, https://doi.org/10.1016/j.actamat.2010.07.038.